論文の内容の要旨

Chemical Charging of Positive Electrode in Fuel Cell/Battery Systems

(燃料電池・蓄電池（FCB）システムにおける正極の化学充電に関する研究)

ムセル　マイク　イグナズ

1. Introduction

The fuel cell/battery (FCB) system was introduced previously by our group[1]. Briefly, the FCB system can run according to three different modes: (i) fuel cell mode, (ii) battery mode, and (iii) FCB mode. Metal hydride (MH) was chosen as the negative electrode and MnO_2 as the positive electrode. In fuel cell mode, the MH and MnO_2 work as catalysts for proton oxidation and oxygen reduction reaction (ORR), respectively. In battery mode, the MH and MnO_2 are redox cycled according to a secondary alkaline battery. Lastly, in FCB mode, discharged MH and discharged MnO_2 (MnOOH) are chemically charged with hydrogen and oxygen, respectively, followed by electrochemical discharge as in battery mode. This mode allows for a high energy density as found in fuel cells and a high power density as found in batteries. The reactions at the positive electrode are shown in Fig. 1.

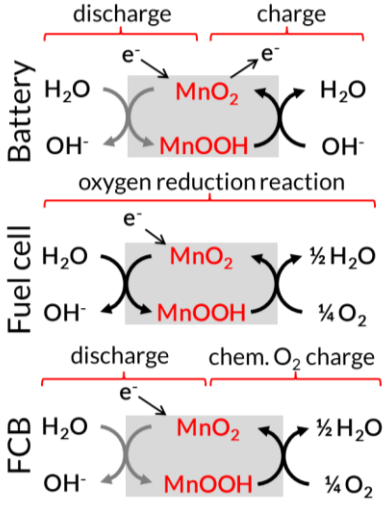

Fig. 1: 3 Different modes in FCB system

It was found that the chemical charging of the MH negative electrode with hydrogen gas is considerably faster than chemical charging of the MnO_2 positive electrode with oxygen gas. Within 10 min, more than 70% of the theoretical capacity of MH was charged with hydrogen gas[2]. In contrast to that, within 1 h only 13% of the theoretical capacity of MnO_2 was charged with oxygen[1]. The focus of this work was therefore the chemical oxygen charging of the positive electrode.

To improve the chemical oxygen charge rate of MnO_2, three steps were undertaken in this dissertation. First, different MnO_2 crystal structures were synthesized and their applicability as positive electrode material were assessed by measuring the capacity and structural stability. Secondly, two of the most stable structures, namely γ- and λ-MnO_2, were used to analyze (a) the chemical oxygen charging mechanism and (b) the effect of different physical properties of MnO_2 on the chemical oxygen charge rate. Based on these findings, in the third part, novel active materials and an electrode with an alternative design were fabricated in order to accelerate the chemical oxygen charge rate of MnO_2.

2. Synthesis and Electrochemical Properties of Different MnO_2 Crystal Structures

Different MnO_2 structures were synthesized in a redox reaction between sodium permanganate and manganese sulfate. α-, β-, γ-, and δ-MnO_2 could be obtained by altering the amount of potassium ion additive and synthesis temperature. As a reference, commercial γ- and λ-MnO_2 were used.

The different MnO_2 crystal structures were analyzed during electrochemical redox cycling (battery mode) to identify the capacity and stability of different structures. It was found that α-MnO_2 was

unsuitable for FCB systems due to transformation into non-rechargeable Mn_3O_4. β-MnO_2 was fairly stable, however, its capacity was low. γ-MnO_2 showed the highest capacity and reasonable crystal stability. δ-MnO_2 had a low capacity and it was found to disintegrate from the binder. λ-MnO_2 showed the best crystal stability and a reasonably high capacity. Thus, γ- and λ-MnO_2 were used in the following parts to analyze the chemical oxygen charge mechanism and assess the effect of the physical properties of MnO_2.

3. Chemical oxygen charging mechanism

3.1. Elucidation of mechanism

To analyze the chemical oxygen charge mechanism, the γ- and λ-MnO_2 electrodes were first fully discharged electrochemically and then chemically charged with oxygen at 1.0 MPa for 1 h. During chemical charging, the potential was measured and compared with electrochemical charge curves. By comparing these curves, the charge capacity during oxygen charge could be deducted. The deviations of these curves were then calculated in order to analyze how the charge rate changes throughout the chemical oxygen charging step. The results are shown in Fig. 2.

During chemical oxygen charging, three stages were considered, namely oxygen adsorption (stage 0), surface charging (stage 1), and proton diffusion from bulk to surface (stage 2) to allow for a complete charge of MnOOH. The chemical oxygen charge rate can be evaluated according to following equation:

$$r = \frac{d[MnO_2]}{dt} = -\frac{d[MnOOH]}{dt} = k\,[MnOOH]^n[O_2]^m \qquad (1)$$

In stage 0, oxygen dissolved, diffused and adsorbed onto the MnO_2 particles. This stage was typically very noisy and because it took several tens of seconds until the system reached a steady-state (constant pressure and oxygen flow), this stage was not analyzed in depth. In stage 1, a constant charge rate was observed, which, according to eq. (1), means that the availability of MnOOH and O_2 at the surface was constant. It is thus suggested that in stage 1, the proton diffusion from the bulk and oxygen diffusion from the electrolyte was sufficiently fast, meaning that the rate limiting step in stage 1 was the reaction rate at the surface. In stage 2, the chemical oxygen charge rate decreased which means that the availability of MnOOH at the surface decreased. It is thus likely that the proton diffusion from the bulk was no longer sufficiently fast to sustain a constant availability $MnOOH_{surf}$, thus slowing the overall reaction down and making proton diffusion the rate determining step. The suggested chemical charge mechanism is shown in Fig. 3.

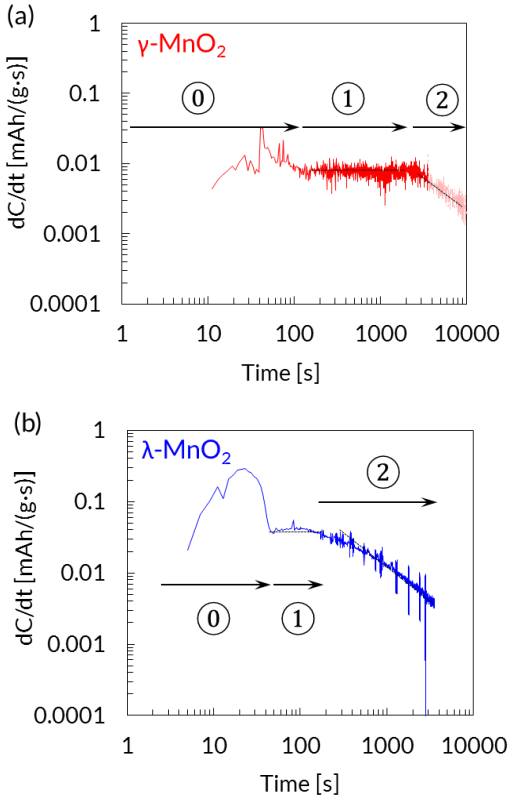

Fig. 2: Change in charge rate of (a) γ-MnO2 and (b) λ-MnO_2 during chemical charging with oxygen, showing three distinct stages.

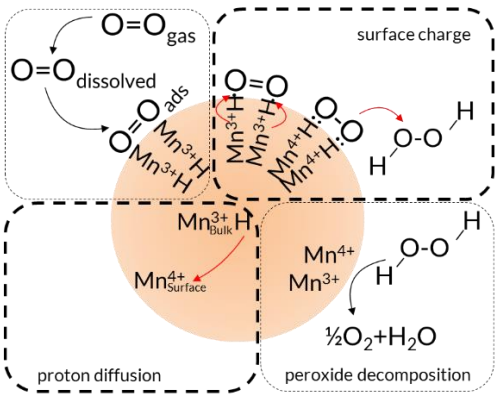

Fig. 3: Suggested chemical oxygen charge mechanism of MnO_2

3.2. Surface oxidation and proton diffusion

Although the chemical oxygen charge curves of γ- and λ-MnO_2 both showed three distinct stages, considerable differences were observed. In stage 1, the chemical charge rates were 8 mAh/(g·s) and 40 mAh/(g·s) for γ-MnO_2 and λ-MnO_2, respectively. Because the surface area of λ-MnO_2 (14.5 m^2/g) was considerably smaller than that of γ-MnO_2 (51.5 m^2/g), the surface specific chemical charge rate of λ-MnO_2 was by a factor of 17.5 higher than that of γ-MnO_2. The reason for the much faster surface charge rate was suggested to be two-fold. Firstly, with X-ray spectroscopy analysis, it was found that γ-MnO_2 underwent strong distortion upon proton intercalation (mainly due to Jahn-Teller distortion) which is known to increase the charge transfer resistance[3]. In contrast to that, only very limited geometrical distortion was found in λ-MnO_2. This resulted in a low charge transfer activation energy in λ-MnO_2, which was calculated by measuring electrochemical impedance spectroscopy (EIS) at different temperatures and applying the Arrhenius function. Secondly, the O–H bond length in λ-MnO_2 is much longer (=weaker) than in γ-MnO_2, which lead to easily removable protons from the λ-MnO_2 lattice and thus boosted the surface charge rate. The surface activity was then analyzed under fuel cell mode in order to verify these observations. As shown in Fig.4, the oxygen reduction reaction (ORR) measurement confirmed that the surface activity of λ-MnO_2 was higher than that of γ-MnO_2.

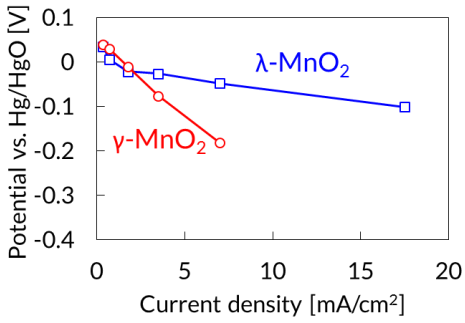

Fig. 4: I-V curve of γ- and λ-MnO_2

Figure 2 also shows that γ-MnO_2 moved from stage 1 to stage 2 much later than λ-MnO_2, which indicated a slower proton diffusion of the latter. The proton diffusion, which was assessed by calculating A√D, could be quantified via EIS analysis. γ-MnO_2 was found to have a 1.7 times faster proton diffusion than λ-MnO_2. This difference was mainly due to the higher surface area in γ-MnO_2. Also this result was verified via an alternative mode, namely battery mode. During electrochemical cycling at high C-rates, shown in Fig. 5, γ-MnO_2 showed considerably better performance at high C-rates which thus confirmed the higher proton diffusion in γ-MnO_2.

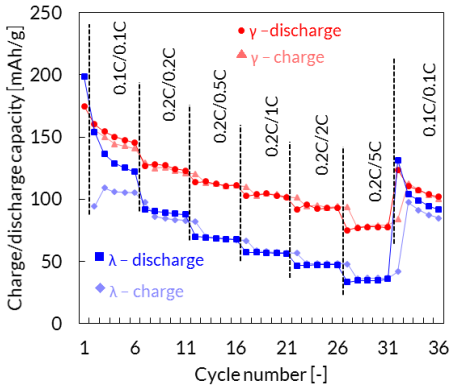

Fig. 5: Electrochemical charge/discharge capacity of γ- and λ-MnO_2 under battery mode

4. Performance Enhancements

4.1. Nano-sized λ-MnO_2 positive electrode

Based on these observations, λ-MnO_2 was identified as the most promising material and its drawback, slow proton diffusion, was overcome by synthesizing samples with short diffusion paths (i.e. high surface area). Micro λ-MnO_2 (23.1 m^2/g) and nano λ-MnO_2 (77.1 m^2/g) were synthesized with a hydrothermal transformation method and a combustion method, respectively. As reference, commercial λ-MnO_2 (14.5 m^2/g) was used. The electrochemical discharge curves after 1 h chemical charging with oxygen are shown in Fig. 6, which show that increasing the surface area of λ-MnO_2 was a very

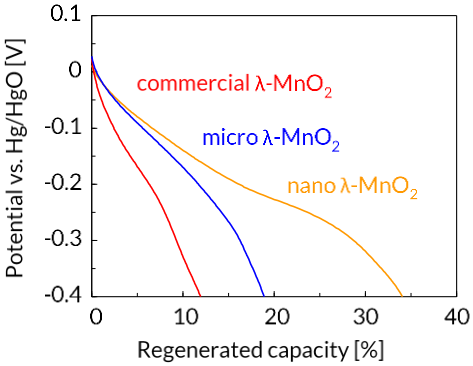

Fig. 6: Electrochemical discharge curves of different samples after 1 h O_2 charge at 1.0 MP

effective way to accelerate the chemical charging rate with oxygen. In addition to that, it was found that the increased surface area improved the ORR rate, capacity, and electrochemical cycling at high C-rates.

4.2. Alternative electrode designs

Lastly, the possibility of using an alternative electrode structure, namely fibrous electrodes, was analyzed. In contrast to pasted electrodes, where binder may cover some of the MnO_2 surface and therefore lower the availability of active sites for chemical charging, in fibrous electrodes, the entire surface of the electroactive material was exposed to the electrolyte which was expected to result in fast chemical oxygen charge rate. Thus, λ-MnO_2-covered carbon fibers (CF) were synthesized by first depositing γ-MnO_2 onto CF, followed by hydrothermal transformation into $LiMn_2O_4$ and subsequent delithiation. It was found that the resulting electrodes could be chemically charged with oxygen to 49.1% of the theoretical capacity within 1 h, as shown in Fig. 7.

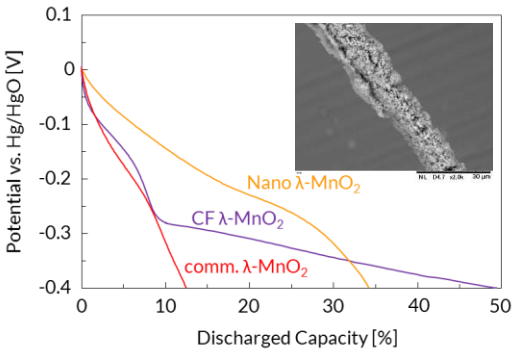

Fig. 7: Electrochemical discharge curves after 1 h chemical oxygen charging. SEM images shows λ-MnO_2 covered carbon fiber

However, the discharge potential was comparatively low and also during electrochemical cycling a high loss was identified. Scanning electron microscopy analysis revealed a poor contact between electroactive material and CF which likely caused high ohmic losses. Future work will therefore have to improve the contact between γ-MnO_2 and CF. Nevertheless, this structure consisting of λ-MnO_2 and CF showed the fastest chemical charge rate to date and is therefore a promising structure for future work.

5. Summary and Outlook

λ-MnO_2 was identified as a possible alternative to γ-MnO_2 for application as positive electrode in FCB systems. Analysis of the physical properties revealed that strong structural stability of the λ-structure and weak O–H bonds are highly beneficial properties for chemical oxygen charging. Thus, λ-MnO_2 was used in subsequent chapters and the performance was improved by synthesizing nano-sized λ-MnO_2, which was found to be rapidly chargeable with oxygen and showed high ORR. The chemical charge rate could further be improved by a fibrous structure which showed a rapid oxygen charge rate.

In future work, a better understanding of the degeneration mechanism of nano λ-MnO_2 has to be gained and methods to inhibit this process need to be found. This may be achieved by doping of λ-MnO_2, improved electrode compositions and, in case of fibrous structures, novel synthesis methods.

References

1. Choi, B., Lee, S., Fushimi, C. & Tsutsumi, A. Power generation/energy storage by a fuel cell/battery system: Regeneration of the MnO2 positive electrode with gaseous oxygen. *Electrochim. Acta* **55,** 8771–8778 (2010).

2. Choi, B., Lee, S., Kawai, H., Fushimi, C. & Tsutsumi, A. Rapid hydrogen charging on metal hydride negative electrode of Fuel Cell/Battery (FCB) systems. *Int. J. Hydrogen Energy* **34,** 2058–2061 (2009).

3. Qu, D. Application of a.c. impedance technique to the study of the proton diffusion process in the porous MnO2 electrode. *Electrochim. Acta* **48,** 1675–1684 (2003).